

Enhanced Laminate Damping via Modification of Viscoelastic Interlayer

FU-SEN LIAO,* TZU-CHIEN J. HSU,[†] and A. C. SU

Institute of Materials Science and Engineering, National Sun Yat-Sen University, Kaohsiung 804, Taiwan, Republic of China

SYNOPSIS

This study sought to develop a sandwich-type vibration damping laminate suitable for room-temperature applications. The laminate consisted of a polymeric interlayer that was sandwiched between two steel sheets. The study was initiated to promote the relatively low-damping capability of a maleic anhydride-grafted polypropylene (mPP)-based laminate, which failed to meet the requirement that the loss factor of the laminate should be greater than 0.05 for effective damping. Modifications of mPP by incorporation of a dynamically vulcanized PP/butyl rubber blend were then followed. The modifications were based on the theoretical analysis proposed by Rose, Ungar, and Kerwin (RUK) for a general polymer-based laminate. The design criteria for the polymeric interlayer, i.e., the preferred range of storage modulus G' for a set of reasonable values of loss tangent ($\tan \delta$), were first established from calculations by use of the RUK theory. The theoretical calculations revealed that the low damping of the mPP-based laminate resulted primarily from the high G' and low $\tan \delta$ of the interlayer. Incorporation of butyl rubber into the polymeric interlayer led to a strong decrease in G' and a moderate increase in $\tan \delta$. These modifications resulted in significantly improved damping capability of the laminate, as predicted by the RUK theory. © 1993 John Wiley & Sons, Inc.

INTRODUCTION

Polymer-laminated steel sheets or polymer/steel laminates, consisting of a thin polymeric interlayer that is sandwiched between two steel sheets, have been used as vibration damping materials in recent years.^{1,2} It is well established that the shear deformation of the viscoelastic interlayer dominates the damping properties in this type of damper.³⁻⁵ Various polymeric interlayers have been considered in the past, including acrylates,⁶ polybutyrals,^{7,8} urethane/acrylate interpenetrating polymer networks (IPNs),⁹ and acrylate/acrylate IPNs.¹⁰

Previous studies indicated that the loss tangent ($\tan \delta$) of the interlayer is of greatest importance.^{11,12} Ross, Ungar, and Kerwin³⁻⁵ (RUK) developed a

theoretical model to calculate the damping capability (indicated in terms of loss factor) of laminate. Based on the RUK model, Chen et al.⁷ investigated the fundamental damping mechanism of the polymer-laminated steel sheet (hereafter, the laminate) as well as variables affecting the damping efficiency. Liao and Hsu⁸ further applied the time-temperature superposition principle to the interlayer in order to obtain high-frequency rheological data from low-temperature measurement to account for the apparent discrepancy⁷ between experimental data and the predictions from the RUK model. This discrepancy was found primarily due to the difference in the frequency applied.⁸ It was observed that^{7,8} the peak damping temperature of a polymer-laminated steel sheet measured using a frequency analyzer in the frequency range from 100 to 1600 Hz would be generally 15–30°C higher than the glass transition temperature (T_g) of the interlayer measured by use of a dynamic rheometer at 1 Hz.

In this study, efforts were concentrated on the development of a vibration damping laminate for

* Also at New Materials R&D Department, China Steel Corporation, Kaohsiung 812, Taiwan, R.O.C.

[†] To whom correspondence should be addressed.

room-temperature applications. Isotactic polypropylene (PP), with its T_g in the neighborhood of 0°C , was chosen as the starting material for the interlayer. PP-based laminates have been developed in recent years for automobiles.¹ However, adhesion between PP and steel is very weak. In practice, this can be overcome by the use of maleic anhydride-grafted PP (mPP). As for the damping capability, the reported loss factor ($\eta = \text{ca. } 0.01$) of the modified PP-based laminate was too low for efficient damping¹; a loss factor greater than 0.05 is generally required for a practical damping application.

To promote the damping capability of the mPP-based laminate, the mPP used had to be further modified. Based on the RUK theory, damping characteristics of the polymer-laminated steel sheet was first simulated in this study. The results led to design criteria for the polymeric interlayer, i.e., the preferred range of storage modulus G' for reasonable $\tan \delta$ values. Results of our theoretical analysis not only provided reasons of the poor damping capability of the mPP-based laminate, but also pointed to the incorporation of rubber to modify the mPP layer.

Butyl rubber (isobutylene-isoprene rubber, IIR) possesses a unique property of high-energy absorption over a wide temperature range¹³ and is frequently utilized as vibration isolators. Its dynamically vulcanized blends (DVB) with polyolefins yield a family of thermoplastic elastomers. These blends consist of a dispersed rubber domain in the polyolefin matrix.¹⁴ A comprehensive review that summarizes the development of the thermoplastic elastomers over the last three decades can be found in the literature.¹⁵ Dynamically vulcanized blends consisting of EPDM elastomers and PP have also been intensively studied by Coran and Patel.¹⁶ In general, DVB behaves like a vulcanized rubber at ambient temperature and can be melt-processed at high tem-

perature as can thermoplastics. They can also be extruded into films without significant changes in phase morphology. Based on property and processibility considerations, we expected that the dynamically vulcanized blend of PP and IIR could be a potential candidate for interlayer material. The modifications of mPP made by the incorporation of butyl rubber to form DVB were then performed and the damping capability of the DVB-based laminates was investigated.

THEORETICAL ANALYSIS

According to the RUK analysis, the loss factor η of a polymer-based laminate, schematically illustrated in Figure 1, can be expressed by³

$$\eta = XY \tan \delta / [1 + (2 + Y)X + (1 + Y)(1 + \tan^2 \delta)X^2] \quad (1)$$

where X is the shear parameter; Y , the stiffness parameter of the laminate; and $\tan \delta$, the loss tangent of the viscoelastic interlayer. The shear parameter X is defined as

$$X = G'[(E_1 H_1)^{-1} + (E_3 H_3)^{-1}] / p^2 H_2 \quad (2)$$

where E is the Young's modulus; H , the thickness; G' , the shear storage modulus of the viscoelastic interlayer; and p , the wave number of the laminate at the resonance frequency. Subscripts 1, 2, and 3 refer, respectively, to individual layers as indicated in Figure 1. Both $\tan \delta$ and G' are functions of temperature. The wave number p is related to resonance frequency according to

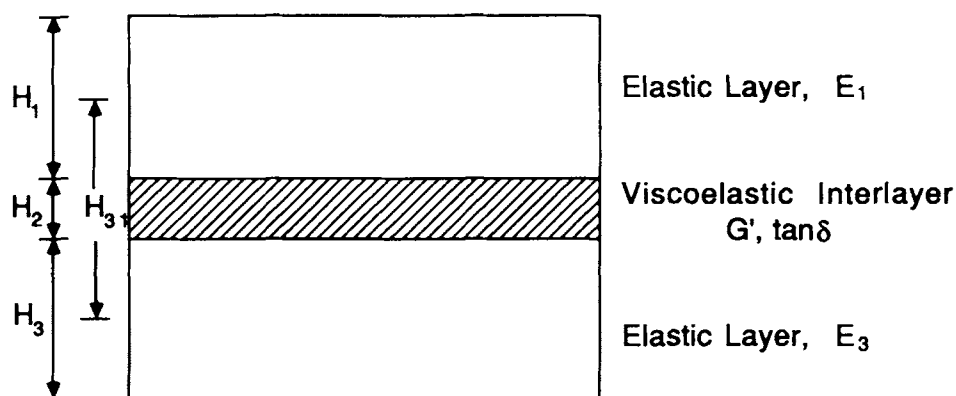


Figure 1 Schematic diagram illustrating the lamination configuration.

$$f_n = (B/\mu)^{1/2} p^2 / 2\pi \quad (3)$$

where f_n is the resonance frequency of the n -th mode; B , the flexural rigidity; and μ , the mass per unit area of the laminate. The stiffness parameter Y is given by

$$Y = 12H_{31}^2 / (E_1H_1^3 + E_3H_3^3) [(E_1H_1)^{-1} + (E_3H_3)^{-1}] \quad (4)$$

where H_{31} is the distance between the neutral planes of the two elastic layers.

For a symmetric laminate with constant thickness of each layers, as in the present case, the stiffness parameter Y is a constant and the shear parameter X is proportional to (G'/p^2) . In addition, it can be shown from eq. (1) that, with constant $\tan \delta$ and Y , there exists an optimal shear parameter X_{opt} where η attains a maximum. Furthermore, η increases with decreasing X value when X is larger than X_{opt} and decreases when X is smaller than X_{opt} .

For a given polymeric interlayer material, it can be seen from eq. (3) that the wavenumber is, to a good approximation, a function of resonance frequency only and can be expressed by $p = p(f_n)$. In this case, the shear parameter is then in the form of

$$X = AG'/p^2(f_n) \quad (5)$$

where A is a constant depending on the laminate configuration and the elastic modulus of steel sheet. Thus, η can be calculated via eq. (1) using selected values of f_n , G' , and $\tan \delta$, i.e.,

$$\eta = \eta(f_n, G', \tan \delta) \quad (6)$$

EXPERIMENTAL

Materials Used and Sample Designation

Materials used in this study included 0.50 mm-thick steel sheets and 0.12 mm-thick polymeric interlayer films. The raw steel sheet was cold-rolled steel (SPCC, China Steel). Two series of polymeric interlayers, designated as the PI series and the DVB series, were prepared. The PI series were dynamically vulcanized blends consisting of an isotactic polypropylene (PP, grade 6331, Taiwan Polypropylene) and a butyl rubber (isobutylene-isoprene rubber or IIR, butyl 402, Polysar). Compositions of the PI series were PP/IIR = 50/50 (PI-50) and 85/15 (PI-85) by weight. Given in Table I is the recipe

Table I Recipe of the PI Series

Ingredient	Weight Ratio
PP	100.0X
IIR	100.0Y
ZnO	5.0Y
Stearic acid	2.0Y
TMTD	1.0Y
MBTS	0.5Y
Sulfur	2.0Y

The ratio X/Y indicates the blend ratio of PP/IIR by weight.

of the PI series. The ingredients zinc oxide and stearic acid were activators for vulcanization; tetramethylthiuram disulfide (TMTD) and 2,2'-dithiobisbenzothiazole (MBTS) were accelerators, and sulfur was the curing agent.

The DVB series consisted of two components denoted as DVB and mPP. Component DVB (Trefsin[®], code no. MDE 553-55A.01, Exxon Chemical Co.) was a dynamically vulcanized blend of PP and IIR; it was used as received. According to the supplier, DVB by itself contained 50–60 wt % of vulcanized IIR, the rest being PP and other minor ingredients not disclosed. The other component mPP (Admer[®], QE-050, Mitsui Petrochemical Co.) was a maleic anhydride-grafted PP. The purpose of adding mPP was to strengthen the adhesion between the interlayer and the steel sheet. Compositions of the DVB series were mPP/DVB = 17/83 (DVB-17) and 8/92 (DVB-8) by weight. Sample designations and blend compositions of these two series are summarized in Table II.

Sample Preparation

A laboratory-scale internal mixer (Plasti-corder PL2000, Brabender) equipped with a pair of high-shear rotors was used to prepare the blends. The rotor rate was kept at 80 rpm throughout the melt-mixing process. The mixing chamber was preheated to 180°C before loading.

Mixing Procedure

For the PI series, ingredients PP, IIR, zinc oxide, and stearic acid were fed sequentially into the mixing chamber at an interval of 30 s. After 3 min of melt mixing, TMTD and MBTS were added, followed by the addition of sulfur 30 s later. Because of the cross-linking reaction in the rubber (dynamic vulcanization and blending), the applied torque raised and

Table II Sample Designations and Blend Compositions

Sample Designation	Composition (Wt. %)			
	PP	IIR	mPP	DVB
PP	100	—	—	—
PI-85	85	15	—	—
PI-50	50	50	—	—
mPP	—	—	100.0	—
DVB-17	—	—	16.7	83.3
DVB-8	—	—	8.3	91.7
DVB	—	—	—	100.0

attained a peak value. Mixing was then continued for 3 more minutes after the maximum torque. For the DVB series, mPP was first introduced into the chamber, followed by the addition of component DVB. Mixing was continued for 3 more minutes beyond the mixing torque maximum.

Compression Molding

After melt mixing, the melt samples were directly compression-molded using a hot press (Model 30T, Carver) to form thick sheets 3.0 mm in thickness for dynamic rheological measurements. The molded sheets were slowly cooled to room temperature. For comparison purposes, sheets of PP, mPP, and DVB of 3.0 mm thickness were also prepared. The press temperature was 190°C for PP and 180°C for all the others.

Lamination

The laminated steel sheets, consisting of two 0.5 mm-thick steel sheets laminated with a 0.12 mm-thick interlayer, were prepared by compression-molding at 200°C. Dimensions of the laminate for frequency spectrum analysis were 18 cm in length and 1 cm in width. Before testing, the specimens were aged at 50°C for 4 h. Details of the specimen specification and preparation have been reported.⁸

Sample Characterization

Dynamic Rheological Measurements

Dynamic rheological data of the polymeric interlayers, including storage modulus G' , loss modulus G'' , and $\tan \delta$, were obtained using a dynamic rheological analyzer (RDS-II, Rheometrics) at a frequency of 1 Hz and a heating rate of 3°C/min. The shear strain

was set at 0.1% to ensure that it was within the linear viscoelastic region of the polymer measured.

Frequency Spectrum Analysis

Details in the vibration-damping measurement have been given elsewhere.⁸ Generally, four resonance peaks (modes 1–4) can be detected in the frequency of 2–1600 Hz. The high-frequency modes, i.e., modes 2–4, were used here for the calculation of the loss factor.

RESULTS AND DISCUSSION

Damping Properties of mPP-based Laminates

Without anhydride-grafting of PP, the interfacial adhesion between PP and steel sheet is poor; the PP-based laminate can easily disintegrate. This results in an inaccurate damping measurement and may cause a reduced damping efficiency. The incorporation of pendant anhydride groups greatly improves the adhesive strength. Shown in Figure 2 are plots of loss factor of the mPP-based laminate vs. temperature at three resonance modes.

It may be observed that the loss factor η is less than 0.01 for all the three resonance modes. Values of η decrease as temperature is lowered. Above 20°C, η gradually reaches a plateau value and then increases slightly with increasing temperature. In addition, η also increases with increasing resonance frequency. In practice, a loss factor of 0.01 is practically too low a value; a laminate with $\eta > 0.05$ is typically required for efficient damping. If one wants to take advantage of the good adhesive property of mPP while maintaining reasonably efficient damping properties, it is necessary to modify PP in some proper ways.

To provide guideline of the modification of PP, calculations based on the RUK model were performed for various G' - $\tan \delta$ combinations at different frequencies. The calculations took into account the effect of frequency, whereas the temperature effect was implicitly considered. Both frequency and temperature are two of the most important factors affecting the damping efficiency of a laminate. Required combinations (i.e., the “design criteria”) of rheological properties (i.e., G' and $\tan \delta$) allowing $\eta > 0.05$ were then examined.

Design Criteria for the Polymer-based Laminates

To explore the effect of the dynamic mechanical properties of the interlayer on the damping prop-

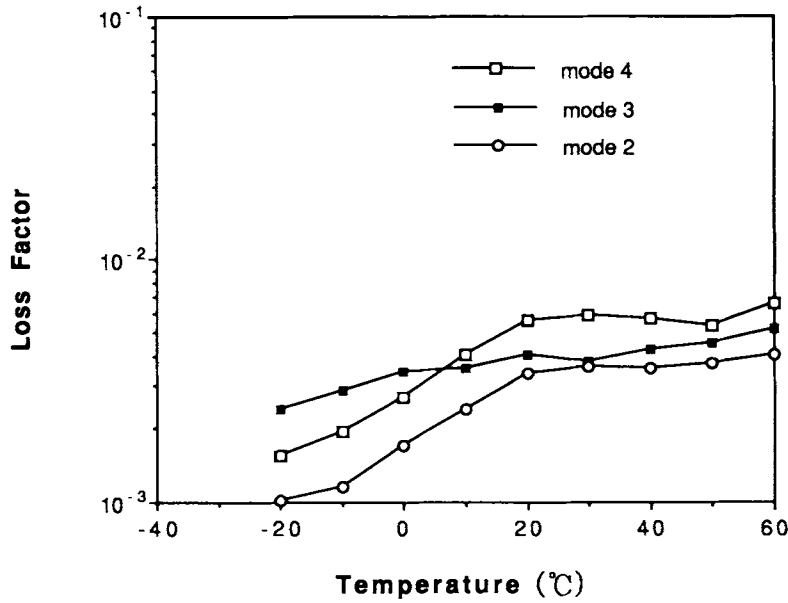


Figure 2 Loss factor of the mPP-based laminate at three resonance frequencies of approximately 200 (mode 2), 500 (mode 3), and 1000 Hz (mode 4).

erties of the laminate, the RUK model was used to predict the loss factor of a symmetrical laminate with the lamination configuration of 0.50/0.12/0.50 mm in thickness. As an example, the calculated loss factor at a resonance frequency of 1000 Hz is plotted against G' for various $\tan \delta$ values in Figure 3.

For each curve of constant $\tan \delta$, there exists a peak where the loss factor reaches maximum at an optimal G' value (G'_{opt}). η increases with increasing

G' when G' is smaller than G'_{opt} , and, on the other hand, η decreases with increasing G' when G' is larger than G'_{opt} . In addition, G'_{opt} varies slightly with $\tan \delta$. As $\tan \delta$ increases, G'_{opt} shifts to a lower value. As may be expected, a higher $\tan \delta$ of the interlayer leads to a higher loss factor. However, it is important to note that, even when $\tan \delta$ is higher than 1.0, there seems no significant improvement on the damping capability at the high G' end. This dem-

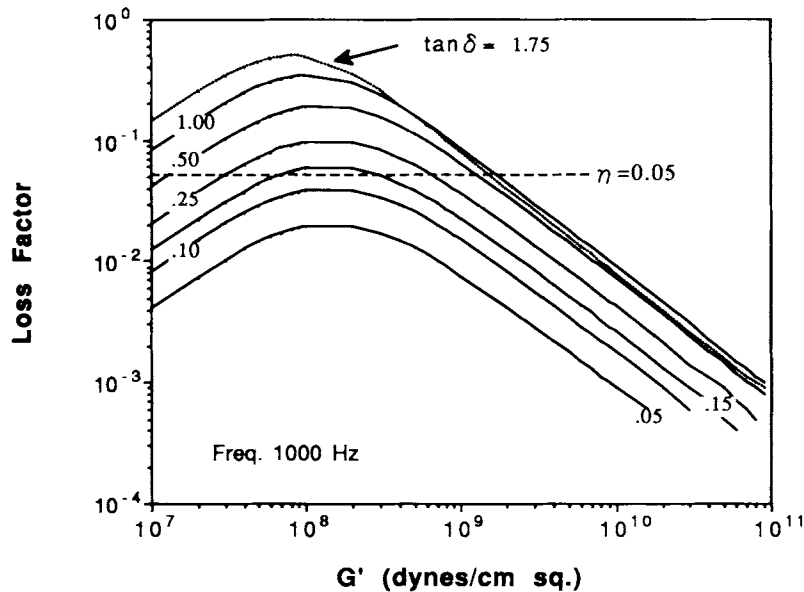


Figure 3 Variation of predicted loss factor with shear storage modulus G' at a resonance frequency of 1000 Hz.

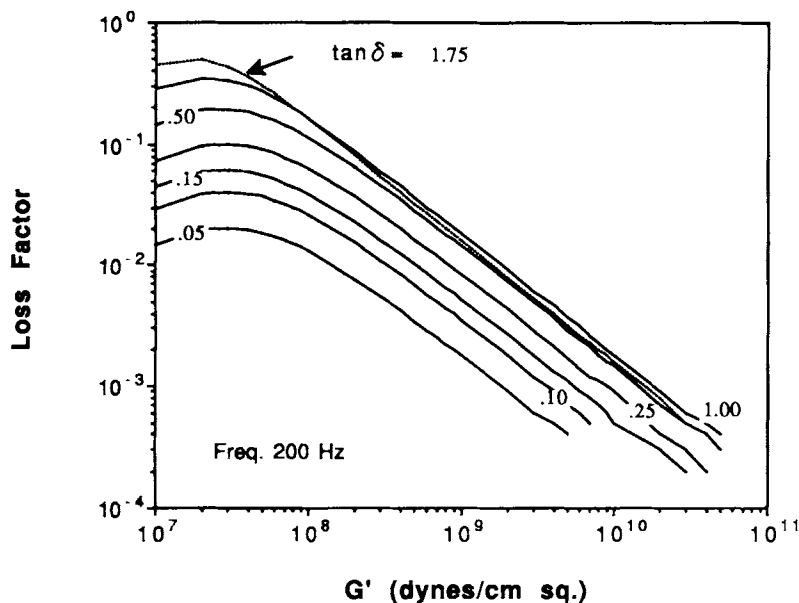


Figure 4 Variation of predicted loss factor with G' at 200 Hz.

onstrates clearly that laminate damping capability is not determined by $\tan \delta$ of the polymer layer alone; the corresponding G' can be important.

The $\tan \delta$ range in Figure 3 has been chosen to be from 0.05 to 1.75. This should encompass typical $\tan \delta$ values of common polymers. Within this range, values of the corresponding G'_{opt} in Figure 3 fall into the range of 8×10^7 to 2×10^8 dynes/cm². It therefore indicates that, in theory, damping of the polymer-based laminate at 1000 Hz will be more efficient if G' of the interlayer can be adjusted to within this optimal range. If one defines $\eta > 0.05$ as the criterion for effective damping of the polymer-laminated steel sheet here, it is evident from Figure 3 that $\tan \delta$ of the interlayer polymer has to be near or above 0.15 (at a frequency of 1000 Hz); the requirements of G' range and G'_{opt} of the same interlayer are thus defined accordingly from Figure 3.

Given in Figure 4 are theoretical predictions at 200 Hz. It is found that these curves are similar to those of 1000 Hz (Fig. 3) in shape but are shifted horizontally to the low G' end. Consequently, G'_{opt} for each constant $\tan \delta$ curve decreases, whereas values of G'_{opt} are shifted to the range of 1×10^7 to 3×10^7 dynes/cm². Similar results for other frequencies can also be obtained. It is generally observed that, for each constant $\tan \delta$ curve, both G' range and the G'_{opt} value decrease with decreasing frequency.

The predicted frequency dependence of G'_{opt} is illustrated in Figure 5, in which the upper and the lower bounds, assigned, respectively, to $\tan \delta = 0.15$

and 1.75, are also indicated. It is observed that G'_{opt} increases with frequency and tends to level off at the high frequency end; the G'_{opt} of the interlayer lies in the range of 1×10^7 to 3×10^8 dynes/cm² for frequencies ranging from 200 to 1600 Hz. Note that since both G' and $\tan \delta$ of the interlayer polymer are functions of temperature the temperature effect is implicitly included in these calculations.

In summary, these calculations indicate that, for the present laminate geometry, it is possible to design a laminate with $\eta > 0.05$ if one can select an interlayer with $\tan \delta > 0.15$ and G' in the vicinity of 10^8 dynes/cm².

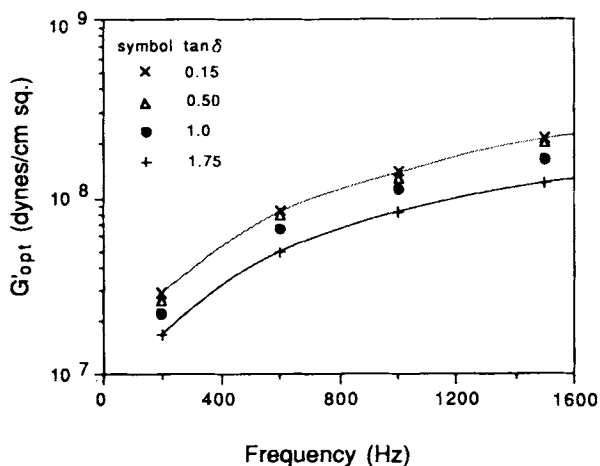


Figure 5 Variation of predicted G'_{opt} with frequency for various $\tan \delta$ values.

Interlayer of Dynamically Vulcanized Blends

The PP interlayer fails to meet the material requirement for effective laminate damping at room temperature in two respects. The first one is its low $\tan \delta$ of 0.07 at its glass transition temperature around 0°C (Fig. 6B). In addition, Figure 6(A) indicates that G' of PP is approximately 10^{10} dynes/cm², a value much too high for damping purposes.

One way to reduce the G' value of the interlayer without shifting of the effective damping temperature range is to introduce a soft, rubbery phase into this layer. As explained in the Introduction, our choice of the soft phase was butyl rubber. Shown also in Figure 6 are dynamic mechanical properties of two dynamically vulcanized PP-IIR blends. The $\tan \delta$ spectra of PI-85 and PI-50 in Figure 6 clearly indicate that the blends are composed of two phases: one is the vulcanized IIR phase with T_g at ca. -60°C and the other is the PP phase with T_g at ca. 0°C . It

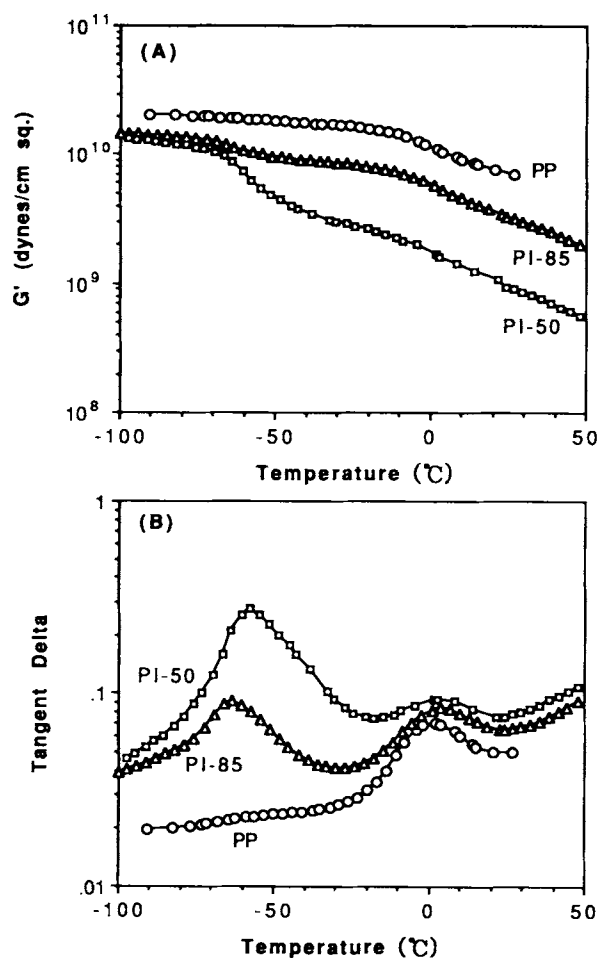


Figure 6 Variation of (A) G' and (B) $\tan \delta$ with temperature for PP, PI-85, and PI-50 at 1 Hz.

is worthwhile to note that G' of PP decays slowly as the temperature is raised from far below its T_g but decreases greatly above T_g . On the other hand, G' of PI-50 and PI-85 decreases remarkably not only around T_g of the PP phase but also in the glass transition region of the rubber phase. Incorporation of the rubber phase into the PP phase effectively decreases G' , especially when the temperature is above the T_g of the rubber phase. Sample PI-50, with a higher rubber content, exhibits a more significant decrease in G' than does sample PI-85. In the vicinity of 0°C , G' decreases from 10^{10} dynes/cm² in the case of neat PP to 10^9 dynes/cm² for PI-50. This decreased value of G' , however, is still an order of magnitude above the estimated optimal G' range.

Samples PI-50 and PI-85 also possess higher $\tan \delta$ in the T_g range of the PP phase. In the vicinity of 0°C , $\tan \delta$ increases from 0.07 in the case of neat PP to 0.09 for PI-50, which is still lower than the theoretically required value of 0.15. This increase of $\tan \delta$ is therefore not significant enough to give an efficient laminate damping.

The viscoelastic behavior of mPP, DVB, and their mechanical blends DVB-8 and DVB-17 are illustrated in Figure 7. Incorporation of mPP in DVB-8 and DVB-17 was to improve their adhesive strength with steel; both are still dynamically vulcanized blends. The mPP shows a T_g approximately at 0°C , with peak $\tan \delta$ of 0.09 and G' of ca. 7×10^9 dynes/cm². No significant difference is observed between the mPP and the neat PP as far as damping capability is concerned, although mPP and PP were obtained from different sources.

The glass transition of the PP phase in the as-received DVB is obscured by the extended loss peak of the IIR phase. In the vicinity of 0°C , $\tan \delta$ is ca. 0.1, whereas G' is ca. 4×10^7 dynes/cm. Judging from theoretical predictions, the former is still low but the latter is in the right range.

Values of shear moduli of samples DVB-8 and DVB-17 lie between those of mPP and the as-received DVB. In the case of DVB-8, the G' value at 0°C is ca. 2×10^8 dynes/cm²; the corresponding $\tan \delta$ value increases slightly after blending. DVB-17, on the other hand, exhibits a rather resolved glass transition around -15°C with a peak $\tan \delta$ of 0.15; its storage modulus at this temperature is 4×10^8 dynes/cm², close to the upper limit of the optimal G' range. The improved $\tan \delta$ of the "overall" PP phase (including mPP and the original PP presented in DVB) in DVB-17 may result from the softening effect due to the presence of the low- T_g rubber phase and from a decreased crystallinity in PP phase due to the incorporation of mPP after mechanical

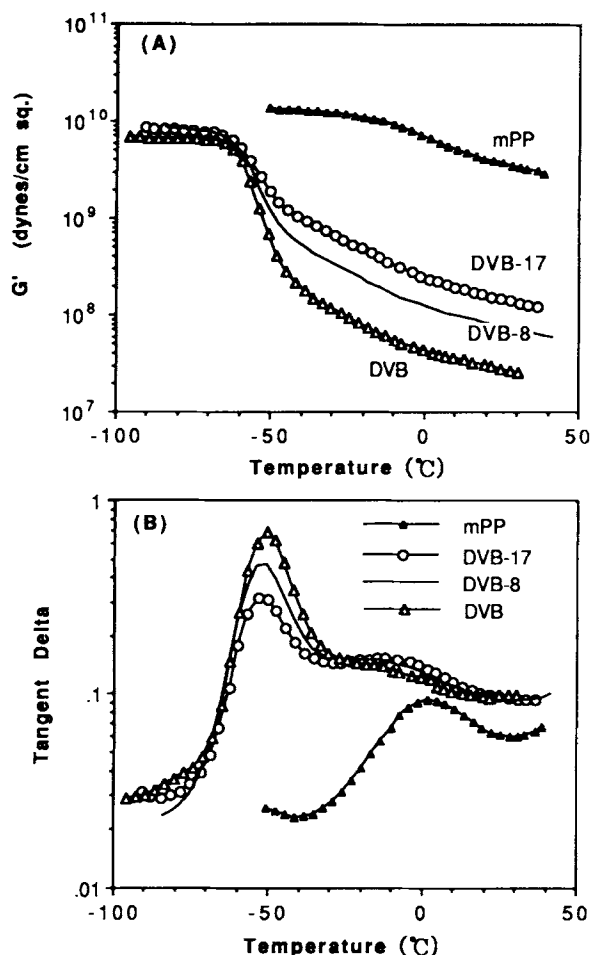


Figure 7 Variation of (A) G' and (B) $\tan \delta$ with temperature for mPP, DVB-8, DVB-17, and DVB at 1 Hz.

blending. According to the preceding calculations, the loss factor of the DVB-17-based laminate may likely reach 0.05.

Comparisons of Damping Efficiency

Given in Figure 8 are results of the vibration damping tests for the mPP-based and DVB-17-based laminates. The measured η of the mPP-based laminate at each resonance mode is smaller than 0.01. The resonance frequency of each mode is quite stable, as indicated in Figure 8(A). In contrast to the glass transition temperature of neat mPP around 0°C, the mPP-based laminate exhibits peak damping between 20 and 30°C. The loss factor at each mode continues to increase as the testing temperature is above 40°C. This may be attributed to the fact that G' of mPP (Fig. 7) decreases continuously with temperature above its T_g .

The measured η of the DVB-17-based laminate

are always greater than 0.01, which are about 1 order of magnitude higher than those of the mPP-based laminate. Unlike the mPP-based laminate, η of the DVB-17-based laminate remains relatively constant in the vicinity of room temperature. Of particular interest is the η of the DVB-17-based laminate at high resonance frequency (mode 4, ca. 1000 Hz); it reaches 0.05 at a temperature of ca. 10°C, approximately 25°C higher than the T_g of the PP phase. According to the theoretical predictions in Figure 3, an interlayer with $\tan \delta$ of 0.15 leads to a loss factor of its corresponding laminate higher than 0.05 (at a frequency of 1000 Hz), if the G' is in the vicinity of 10^8 dynes/cm². Since DVB-17 exhibits a T_g at -15°C with $G' = 4 \times 10^8$ dynes/cm² and $\tan \delta = 0.15$, the theoretical prediction is in good agreement with the experimental observation. At low testing frequencies of modes 2 and 3, the peak damping temperatures of the DVB-17-based lami-

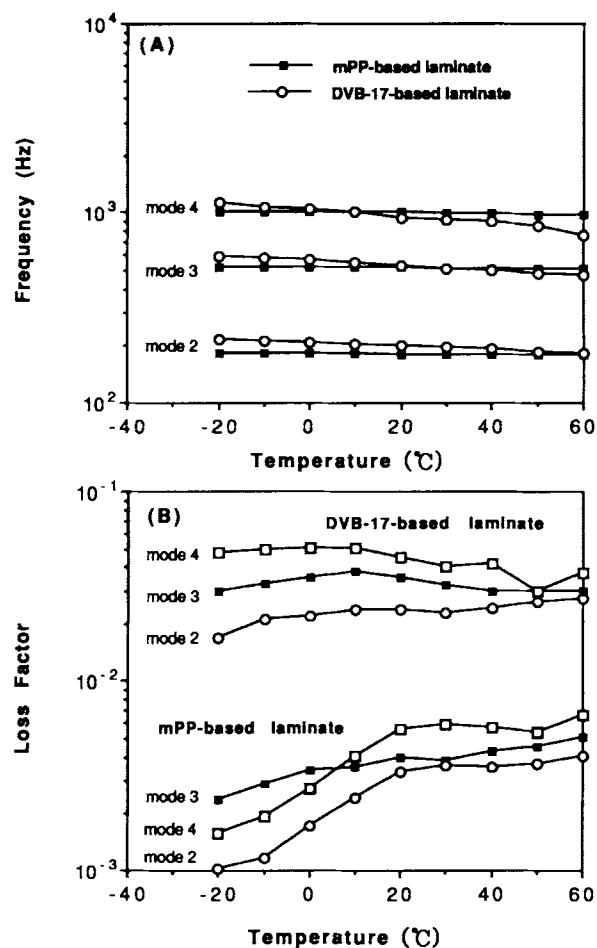


Figure 8 Variation of (A) resonance frequency and (B) loss factor measured with temperature for the mPP-based and the DVB-17-based laminates.

nate are also around 10°C, but η values are somewhat lower, ranging from 0.01 to 0.04. In this respect, there exists space for further improvements.

SUMMARY

We have demonstrated in this study the development of a polymer-laminated steel sheet targeted to be used for room-temperature damping. The study was initiated to improve the relatively low damping capability of the mPP-based laminate. For effective damping, a laminate loss factor greater than 0.05 is highly desirable. The mPP-based laminate failed to meet this goal. Modifications of mPP by incorporation of butyl rubber via a dynamic vulcanization process were then performed. The interlayer polymer used was based on a dynamically vulcanized blend consisting of a PP and a butyl rubber.

The modifications were primarily based on the theoretical calculations according to the model proposed by Rose, Ungar, and Kerwin. In these calculations, the damping efficiency of polymer-laminated steel sheets with a fixed lamination configuration was predicted explicitly in terms of G' and $\tan \delta$ of the interlayer polymer as well as the resonance frequency. The prediction indicated that at a specific frequency and a given $\tan \delta$ value there existed a G'_{opt} where the loss factor η attained its maximum value. At a fixed $\tan \delta$, G'_{opt} decreased with decreasing frequency. In addition, at a specific frequency, G'_{opt} varied just slightly with $\tan \delta$ of the interlayer. For the loss factor of a laminate to be greater than 0.05 in the frequency of 200–1600 Hz, the requirements of the interlayer polymer that $\tan \delta > 0.15$ and $1 \times 10^7 < G'_{\text{opt}} < 3 \times 10^8$ dynes/cm² were established from the theoretical predictions.

The calculations also revealed that the low damping of the mPP-based laminate was due mainly to its high G' and low $\tan \delta$. Incorporation of a dis-

crete butyl rubber phase into PP via a dynamically vulcanized blend led to a strong decrease in G' and a moderate increase in $\tan \delta$, resulting in significant improvement in laminate loss factor that compared favorably with the theoretical prediction.

REFERENCES

1. A. Jouet and M. Glemet, in *Hot & Cold-Rolled Sheet Steels*, R. Pradhan and G. Ludkovsky, Eds., TMS, Warrendale, PA, 1988, p. 221.
2. N. Chiba, *Nippon Kokan Techn. Rep.* (Fukuyama, Japan), **43**, 50 (1985).
3. D. Ross, E. E. Ungar, and E. M. Kerwin, Jr., in *Structural Damping*, J. E. Ruzicka, Ed., ASME, New York, 1959, Sec. 3.
4. E. M. Kerwin, Jr., *J. Acoust. Soc. Am.*, **31**, 952 (1959).
5. E. E. Ungar, *J. Acoust. Soc. Am.*, **34**, 1082 (1962).
6. J. A. Grates, J. E. Lorenz, D. A. Thomas, and L. H. Sperling, *Mod. Paint Coat.*, **Feb.**, 35 (1975).
7. Y. S. Chen, T. J. Hsu, and S. I. Chen, *Metall. Trans.*, **22A**, 653 (1991).
8. F. S. Liao and T. J. Hsu, *J. Appl. Polym. Sci.*, **45**, 893 (1992).
9. C. J. Tung and T. J. Hsu, *J. Appl. Polym. Sci.*, to appear.
10. J. A. Grates, D. A. Thomas, E. C. Hickey, and L. H. Sperling, *J. Appl. Polym. Sci.*, **19**, 1731 (1975).
11. D. I. G. Jones, *J. Sound Vibration*, **33**, 451 (1974).
12. H. Mizumachi, *J. Adhesion*, **2**, 292 (1970).
13. K. J. Kumbhani and E. G. Kent, *Rubber World*, **Apr.**, 43 (1982).
14. R. C. Puydak and D. R. Hazelton, *Plast. Eng.*, **Sept.**, 37 (1988).
15. N. R. Leege, *Rubber Chem. Technol.*, **62**, 529 (1989).
16. A. Y. Coran and R. Patel, *Rubber Chem. Technol.*, **53**, 141 (1980).

Received February 19, 1992

Accepted September 16, 1992